

Slim LSTM NETWORKS: LSTM_6 and LSTM_C6

Atra Akandeh and Fathi M. Salem

Circuits, Systems, and Neural Networks (CSANN) Laboratory
Computer Science and Engineering || Electrical and Computer Engineering
University Neuroscience Program
Michigan State University
East Lansing, Michigan 48864-1226
akandeha@msu.edu; salemf@msu.edu

Abstract—We have shown previously that our parameter-reduced variants of Long Short-Term Memory (LSTM) Recurrent Neural Networks (RNN) are comparable in performance to the *standard LSTM RNN* on the MNIST dataset. In this study, we show that this is also the case for two diverse benchmark datasets, namely, the review sentiment IMDB and the 20 Newsgroup datasets. Specifically, we focus on two of the simplest variants, namely LSTM_6 (i.e., *standard LSTM* with three constant fixed gates) and LSTM_C6 (i.e., LSTM_6 with further reduced cell body input block). We demonstrate that these two aggressively reduced-parameter variants are competitive with the *standard LSTM* when hyper-parameters, e.g., learning parameter, number of hidden units and gate constants are set properly. These architectures enable speeding up training computations and hence, these networks would be more suitable for online training and inference onto portable devices with relatively limited computational resources.

Index Terms—Gated Recurrent Neural Networks (RNNs), Long Short-term Memory (LSTM), Keras Library.

1. Introduction

Recurrent Neural Networks (RNNs) have been making an impact in sequence-to-sequence mappings, with particularly successful applications in speech recognition, music, language translation, and natural language processing to name a few [5], [7], [11], [13], [22]. By their structure, they possess a memory (or state) and include feedback or recurrence. The *simple RNN* (sRNN) is succinctly expressed, see e.g., [10]:

$$\begin{aligned} h_t &= \sigma(W_{hx}x_t + W_{hh}h_{t-1} + b_h) \\ y_t &= W_{hy}h_t + b_y \end{aligned} \quad (1)$$

where x_t is the input sequence vector at (time) step t , h_t is the hidden (activation) unit vector at step t , while h_{t-1} is the hidden unit vector at the previous step $t-1$, and y_t is the output vector at step t . The parameters are the three matrices, namely, W_{hx} , W_{hh} , and W_{hy} , and the vector b_h . This constitutes a discrete-step dynamic recurrent

system with h_t acting as the state. The parameters are to be determined adaptively via training mostly using various versions of backpropagation through time (BPTT), e.g., see [11].

The LSTM RNNs introduce a cell-memory and 3 gating signals to enable effective learning via the BPTT [11]. The simple activation state has been replaced with a more involved activation with gating mechanisms. The LSTM RNN uses a (additional) memory cell (vector and includes three gates: (i) an input gate, i_t (ii) an output gate o_t , and (iii) a forget gate, f_t . These gates collectively control signaling. The *standard LSTM* is expressed mathematically as [10], [11]:

$$\begin{aligned} i_t &= \sigma_{in}(W_i x_t + U_i h_{t-1} + b_i) \\ f_t &= \sigma_{in}(W_f x_t + U_f h_{t-1} + b_f) \\ o_t &= \sigma_{in}(W_o x_t + U_o h_{t-1} + b_o) \\ \tilde{c}_t &= \sigma(W_c x_t + U_c h_{t-1} + b_c) \\ c_t &= f_t \odot c_{t-1} + i_t \odot \tilde{c}_t \\ h_t &= o_t \odot \sigma(c_t) \end{aligned} \quad (2)$$

where the first 4 equations are replica of the simple RNN (sRNN) above, with the first 3 equations serving as gating signals and thus their nonlinear activation is set as a sigmoid function σ_{in} , while the 4th equation's nonlinearity is an arbitrary nonlinearity σ , typically sigmoid, hyperbolic tangent (*tanh*), or rectified linear unit (ReLU). This 4th equation is sometimes referred to as the input block. The last two equations entail the memory cell c_t and now activation hidden unit h_t with the insertion of the gating signals in a point-wise (Hadamard) multiplications (using the symbol \odot). This represents a discrete-step nonlinear dynamic system with recurrence. The distinct parameters are associated with each replica as W_* , U_* , and b_* is a straight fashion.

The output layer of the LSTM model may be chosen to be as a linear (more accurately, affine) map as

$$y_t = W_{hy}h_t + b_y \quad (3)$$

where y_t is the output, and W_{hy} is a matrix, and b_y is a bias vector. In other optional implementation, this layer may be

followed by a softmax layer to render the output analogous with probability ranges.

LSTMs are relatively computationally expensive due to the fact that they have four replica with distinct sets of parameters (namely, weights and biases) which would need to be adaptively updated every (mini-batch) of training calculations.

We have introduced numerous, computationally simpler, LSTM variants by aggressively eliminating some of the adaptive parameters, see [1], [2], [3], [14], [16], [20], [21]. In this study we shall focus on one of the simplest variant forms, namely the slim LSTM_6 and LSTM_C6 [2], [21].

2. LSTM_6

Different variants have been introduced earlier [3], [21]. For LSTM_6, the gating signals are set at constant values as follows:

$$\begin{aligned}
 i_t &= 1.0 \\
 f_t &= f, \quad -1 < f < 1.0 \\
 o_t &= 1.0 \\
 \tilde{c}_t &= \sigma(W_c x_t + U_c h_{t-1} + b_c) \\
 c_t &= f_t \odot c_{t-1} + i_t \odot \tilde{c}_t \\
 h_t &= o_t \odot \sigma(c_t)
 \end{aligned} \tag{4}$$

Note that the gate signal values are set to the constant scalars f or 1. In practice, when the gate is set to 1, it is equivalent to eliminating the gate entirely! Thus, in compact form, the LSTM_6 equation now reads:

$$\begin{aligned}
 c_t &= f c_{t-1} + \sigma(W_c x_t + U_c h_{t-1} + b_c), \quad -1 < f < 1.0 \\
 h_t &= \sigma(c_t)
 \end{aligned} \tag{5}$$

This variant form is close to the so-called basic Recurrent Neural Network (bRNN), see [19], [21] for analysis and details.

3. LSTM_C6

In LSTM_C6 the matrix U_c in the cell equation is replaced with a corresponding vector u_c , in order to render a point-wise multiplication instead. This the variant equations become

$$\begin{aligned}
 i_t &= 1.0 \\
 f_t &= f, \quad -1 < f < 1.0 \\
 o_t &= 1.0 \\
 \tilde{c}_t &= \sigma(W_c x_t + u_c \odot h_{t-1} + b_c) \\
 c_t &= f_t \odot c_{t-1} + i_t \odot \tilde{c}_t \\
 h_t &= o_t \odot \sigma(c_t)
 \end{aligned} \tag{6}$$

Similarly, in compact form, these equations now read as:

$$\begin{aligned}
 c_t &= f c_{t-1} + \sigma(W_c x_t + u_c \odot h_{t-1} + b_c), \quad -1 < f < 1.0 \\
 h_t &= \sigma(c_t)
 \end{aligned} \tag{7}$$

To account for the number of parameters in each case, let the input vector x_t be of m dimension, the state c_t and its activation hidden unit has dimension of n . Then the number of (adaptive) parameters in LSTM_6 is $n(m + n + 1)$ and for LSTM_C6 the total number of (adaptive) parameters is $n(m + 2)$. (Note that one may add to each the new nonadaptive *hyper-parameter* f). Thus if the state dimension $n = 100$ and the input dimension is $m = 32$, the total number of (adaptive) parameters for LSTM_6 is 3400.

Table 1 and Table 2 provide a summary of the number of parameters as well as the times per epoch during training corresponding to each of the model variants for $h = 100$ for each data set. The number of parameter only include parameter corresponding to LSTM layer and parameter of embedding and last dense layer is not included. These simulation and the training times are obtained by running the Keras Library [6] with GPU option enable. Although, we expect that LSTM_C6 takes less time per epoch than LSTM6, but due to Keras internal implementation, that is not the case. However, LSTM_C6 is still faster than basic LSTM. Comparing these two table indicate that time-wise, parameter reduction plays a huge role in larger networks.

4. Experiments and Discussion

In the previous work [2], we have shown that our networks are competitively comparable to *standard* LSTM networks on the MNIST dataset. Here we show that LSTM_6 (also denoted here as LSTM6) and LSTM_C6 can compete with the *standard* LSTM network in the benchmark public datasets IMDB and 20 Newsgroup available via the Keras library <https://keras.io>.

4.1. The IMDB dataset

IMDB Datasets is a binary sentiment classification dataset. To train the model, dictionary size of 5000 has been used. Each review is truncated or padded to 500 words. The first layer is an embedding layer which is a simple multiplication that transforms words into their corresponding word embedding. The output is then passed to an LSTM layer following a dense layer. The network specification which has been adopted from Keras 1.2 examples is given in table 3.

A schematic representation of the architecture used is given in figure 1.

TABLE 1: Variants specifications: IMDB Dataset

variants	# of parameters	dimensions
LSTM	53200	m=32, n=100
LSTM6	13300	m=32, n=100
LSTM_C6	3400	m=32, n=100

TABLE 2: Variants specifications: 20 Newsgroup Dataset

variants	# of parameters	dimensions
LSTM	263168	m=128, n=128
LSTM6	65792	m=128, n=128
LSTM_C6	33280	m=128, n=128

TABLE 3: Network specifications: IMDB Datasets

Input dimension	500×32
Number of hidden units	100, 200, 300, 400
Non-linear function	sigmoid
Output dimension	1
Number of epochs	100
Optimizer	Adam
Batch size	32
Loss function	binary cross-entropy

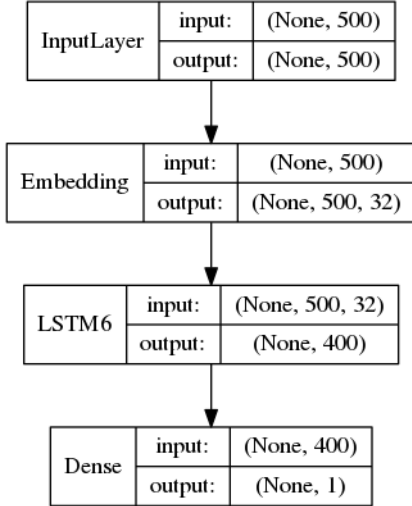


Figure 1: Network Architecture Diagram for IMDB

In this experiment, the *sigmoid* nonlinearity is used, since the *tanh* nonlinearity has caused large fluctuations in training and testing outcomes and using the *ReLU* nonlinearity routinely failed to converge even for the *standard* LSTM RNN.

4.1.1. Tuning the hyper-parameter η . We started with the generic $\eta = 1e-3$ as used in the Keras library example. As it is shown in figure 2, the *standard* LSTM (denoted as *lstm0* in the figure) displays smooth profiles with (testing) accuracy around 88%. However, LSTM_6 (denoted as LSTM6 in the figure) shows fluctuations and also does not catch up with *standard* LSTM. This is an indicator that $\eta = 1e-3$ is too large for this variant network. Since the number of parameters in LSTM6 has aggressively been reduced, it is expected that the different optimal values of η would work better. This is study, we consider a grid of two values around the default value. Decreasing η to $1e-4$ improves the performance of LSTM6 to 82%, however a small amount of fluctuation is still observed. Meanwhile, LSTM_C6 did not show any improvement.

The typical results obtained over the eta-grid among all the epochs are shown in Table 4.

4.1.2. Increasing the dimension of the state or hidden units. To compensate for decreased number of parameters, the dimension of hidden units has been increased along with different smaller values of η . As it is shown, higher dimensions need less epoch to reach leveling off profiles.

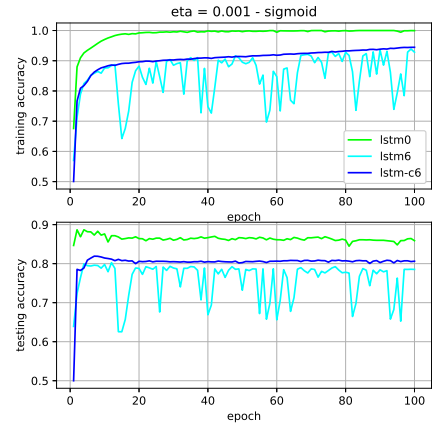


Figure 2: IMDB, Training & Test accuracy, $\sigma = \text{sigmoid}, \eta = 1e-3$

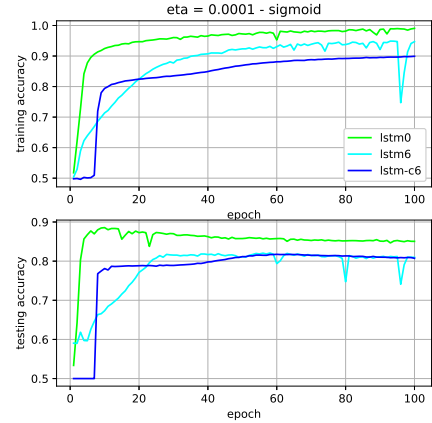


Figure 3: IMDB, Training & Test accuracy, $\sigma = \text{sigmoid}, \eta = 1e-4$

TABLE 4: Best results obtained for IMDB using sigmoid

		$\eta = 1e-4$	$\eta = 1e-3$	$\eta = 2e-3$
LSTM	train	0.9906	1.0000	0.9600
	test	0.8856	0.8868	0.7775
LSTM6	train	0.9489	0.9387	0.7850
	test	0.8208	0.8026	0.7100
LSTM_C6	train	0.8992	0.9445	0.9556
	test	0.8174	0.8192	0.7842

Setting $\eta = 1.25e-5$, creates an almost fluctuation free profile. In the following figures *lstm62* stands for LSTM6 using 200 hidden units.

4.1.3. Tuning the constant forget hyper-paramter. The forget (gate) constant value must be less than one in absolute value for bounded-input-bounded-output (BIBO) stability [19]. In our previous work [3], $f > 0.59$ did not work for the MNIST dataset and training would not converge. In this paper on this different dataset, we initially start with the same value (i.e., $f = 0.59$). To fill in the gap

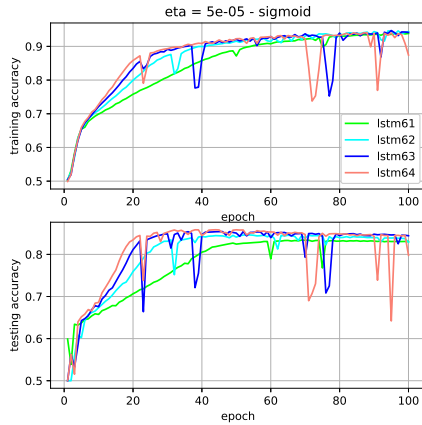


Figure 4: IMDB, Training & Test accuracy, $\sigma = \text{sigmoid}, \eta = 5e-5$

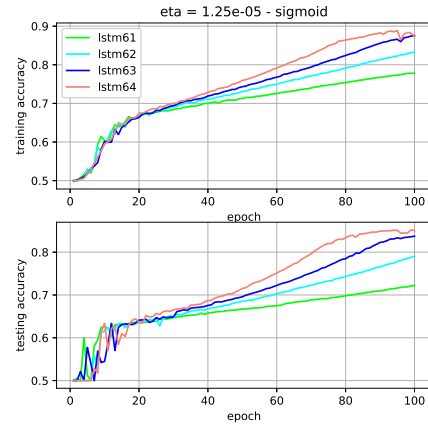


Figure 6: IMDB, Training & Test accuracy, $\sigma = \text{sigmoid}, \eta = 1.25e-5$

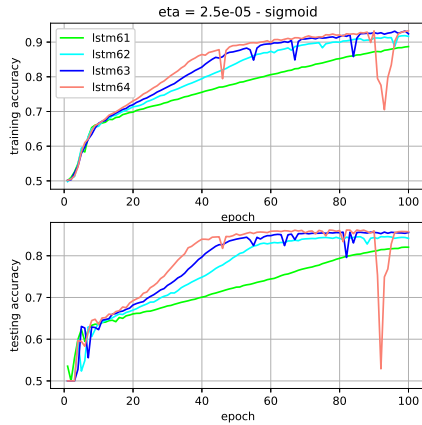


Figure 5: IMDB, Training & Test accuracy, $\sigma = \text{sigmoid}, \eta = 2.5e-5$

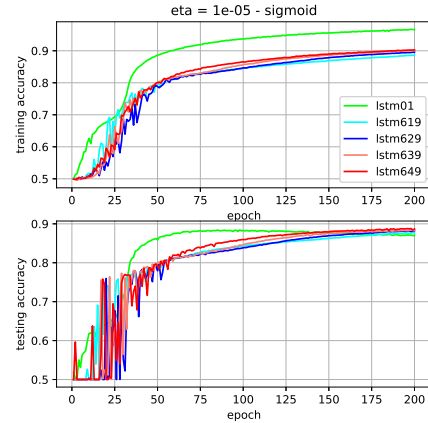


Figure 7: IMDB, Training & Test accuracy, $\sigma = \text{sigmoid}, \eta = 1e-5$

TABLE 5: Best results obtained Using sigmoid.

		$\eta = 5e-5$	$\eta = 2.5e-5$	$\eta = 1.25e-5$
100	train	0.9396	0.8871	0.7783
	test	0.8340	0.8206	0.7219
200	train	0.9461	0.9185	0.833
	test	0.8461	0.8459	0.7908
300	train	0.9471	0.9319	0.8754
	test	0.8542	0.8567	0.8374
400	train	0.9404	0.933	0.8887
	test	0.8585	0.8618	0.8523

between *standard* LSTM and LSTM6, we gradually increase the forget hyperparameter f and observe that IMDB dataset produce BIBO stable performance up to $f_t = 0.96$. Since the accuracy plot profiles show increasing performance trend and do not appear to level off after 100 epochs. We run the training for 200 epochs. It is observed that LSTM6 surpass *standard* LSTM at around epoch 150.

The effect of increasing the hyper-parameter f in the LSTM_C6 network using $h = 200$ and $\eta = e-5$ is also

depicted in figure 8. In this figure, lstm-c6295 denotes LSTM_C6 using $h = 200$ and $f = 0.95$.

4.2. The20 Newsgroups dataset

The 20 Newsgroups dataset is a collection of 20000 documents, containing 20 different newsgroups. GloVe embedding is used to pre-train the model [6]. The network architecture is adapted from Keras1.2 examples. Table 6 provides the network specification. We have applied our variants in the bidirectional layer. A schematic representation of the architecture used is given in figure 9.

4.2.1. The tanh activation. Using *tanh* as nonlinearity, the LSTM_C6 layer results in better performance than using the LSTM6 layer and even using the *standard* LSTM layer. It is observed that setting $\eta = 1e-3$ results in test score of 79.42% in LSTM_C6 which surpasses the test score of the *standard* LSTM, 77.75%, using $\eta = 2e-3$. The best results

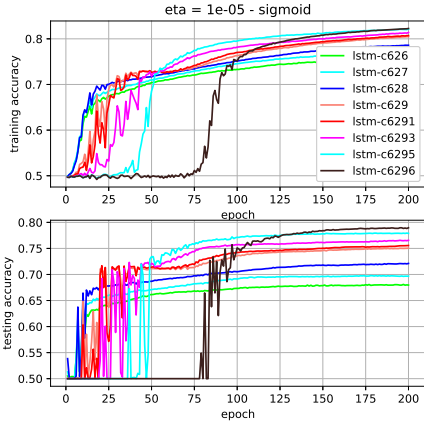


Figure 8: IMDB, Training & Test accuracy, $\sigma = \text{sigmoid}, \eta = 1e-5$

TABLE 6: Network specifications.

Input dimension	1000
Embedding layer	1000×100
Conv1D(128, 5,'relu')	996×128
Maxpooling1D(5)	199×128
Conv1D(128, 5,'relu')	195×128
Maxpooling1D(5)	39×128
Conv1D(128, 5,'relu')	35×128
Maxpooling1D(2)	17×128
Number of epochs	100
Bidirectional(lstm)	256
Dense	128
Dense	6
Optimizer	rmsprop
Batch size	128
Loss function	categorical cross-entropy

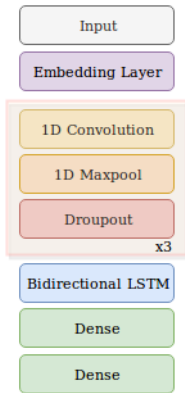


Figure 9: News20, Network Architecture Diagram

obtained for the three grid values of η over 100 epochs are summarized in Table 7.

4.2.2. The (logistic) sigmoid activation. Using *sigmoid* as nonlinearity, the similar trend is observed; LSTM_C6 shows better performance than LSTM6 and even *standard* LSTM.

TABLE 7: Best results obtained for news20 LSTM models

		$\eta = 5e-4$	$\eta = 1e-3$	$\eta = 2e-3$
LSTM	train	0.9519	0.9581	0.9600
	test	0.7592	0.7750	0.7775
LSTM6	train	0.8169	0.8448	0.7850
	test	0.7158	0.7200	0.7100
LSTM_C6	train	0.9552	0.9583	0.9556
	test	0.7792	0.7942	0.7842

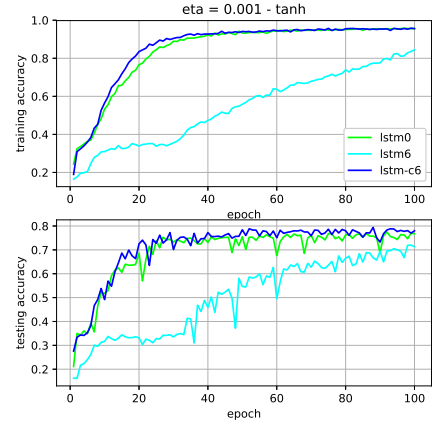


Figure 10: News20, Training & Test accuracy, $\sigma = \text{tanh}, \eta = 1e-3$

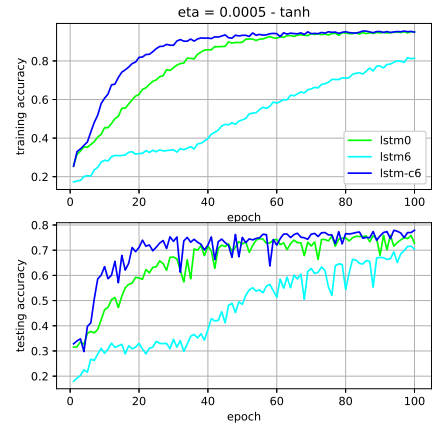


Figure 11: News20, Training & Test accuracy, $\sigma = \text{tanh}, \eta = 5e-4$

5. Conclusion

LSTM_6 and LSTM_C6, which are aggressively reduced variant of the baseline *standard* LSTM have been evaluated on the benchmark classical IMDB and 20 News-groups datasets. In these slim LSTM variants, the gates are set at constants, and effectively only the forget gate serves now as a hyper-parameter to ensure BIBO stability of the discrete dynamic recurrent neural network (RNN). LSTM_C6 further reduced the matrix U_c in the input block equation into a vector with point-wise (Hadamard) multipli-

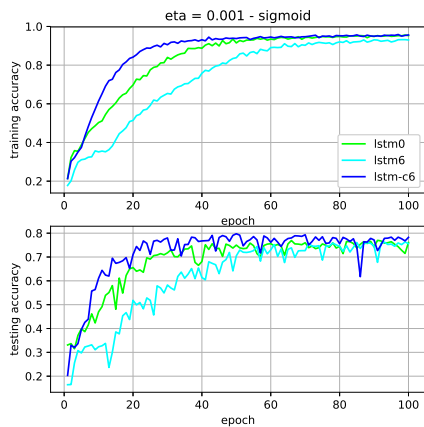


Figure 12: Training & Test accuracy, $\sigma = \text{sigmoid}$, $\eta = 1e-3$

ation. We tried limited grid of 3 values of the learning rate centered around a default value for the *standard* LSTM RNN using in the Keras Library. Moreover, the network dimension can be used as a hyper-parameter to improved the slim LSTM variants. These investigations have shown that the capacity of the slim LSTMs can match the *standard* LSTM while still saving computational expense. It was observed that as we increase the number of hidden units the performance improves. Finally, using the hyper-parameter f in place of the forget gate f_t , the training/ testing performance can also improve, up to to the value $f = 0.96$ for the IMDB dataset. This enables LSTM6 to surpass *standard* LSTM at around 150 epochs. In the 20 Newsgroups dataset, LSTM_C6 surpasses base LSTM without much parameter tuning. As a results we conclude that these simplified models are comparable to the *standard* LSTM. Thus, these slim LSTM variants may be suitably employed in applications in order to benefit from realtime speed and/or computational expense.

Acknowledgment

This work was supported in part by the National Science Foundation under grant No. ECCS-1549517.

References

- [1] A. Akandeh and F. M. Salem. Simplified long short-term memory recurrent neural networks: part I. *arXiv:1707.04619*, 2017.
- [2] A. Akandeh and F. M. Salem. Simplified long short-term memory recurrent neural networks: part II. *arXiv:1707.04623*, 2017.
- [3] A. Akandeh and F. M. Salem. Simplified long short-term memory recurrent neural networks: part III. *arXiv:1707.04626*, 2017.
- [4] Y. Bengio, P. Simard, and P. Frasconi. Learning long-term dependencies with gradient descent is difficult. *IEEE transactions on neural networks*, 5(2):157–166, 1994.
- [5] N. Boulanger-Lewandowski, Y. Bengio, and P. Vincent. Modeling temporal dependencies in high-dimensional sequences: Application to polyphonic music generation and transcription. *arXiv preprint arXiv:1206.6392*, 2012.
- [6] F. Chollet. Keras github. <https://github.com/fchollet/keras/blob/master/examples>.

- [7] J. Chung, C. Gulcehre, K. Cho, and Y. Bengio. Empirical evaluation of gated recurrent neural networks on sequence modeling. *arXiv preprint arXiv:1412.3555*, 2014.
- [8] F. A. Gers, J. Schmidhuber, and F. Cummins. Learning to forget: Continual prediction with lstm. *Neural computation*, 12(10):2451–2471, 2000.
- [9] F. A. Gers, N. N. Schraudolph, and J. Schmidhuber. Learning precise timing with lstm recurrent networks. *Journal of machine learning research*, 3(Aug):115–143, 2002.
- [10] I. Goodfellow, Y. Bengio, and A. Courville. *Deep Learning*. MIT Press, 2016. <http://www.deeplearningbook.org>.
- [11] K. Greff, R. K. Srivastava, J. Koutnk, B. R. Steunebrink, and J. Schmidhuber. Lstm: A search space odyssey. *IEEE transactions on Neural Networks and Learning Systems*, 28(10):2222–2232, 2017.
- [12] S. Hochreiter and J. Schmidhuber. Long short-term memory. *Neural computation*, 9(8):1735–1780, 1997.
- [13] M. Johnson, M. Schuster, Q. V. Le, M. Krikun, Y. Wu, Z. Chen, N. Thorat, F. B. Viégas, M. Wattenberg, G. Corrado, M. Hughes, and J. Dean. Google’s multilingual neural machine translation system: Enabling zero-shot translation. *CoRR*, abs/1611.04558, 2016.
- [14] D. Kent and F. M. Salem. Performance of three slim variants of the long short-term memory (lstm) layer. *arXiv preprint arXiv:1901.00525*, 2019.
- [15] Y. LeCun, C. Cortes, and C. J. Burges. Mnist handwritten digit database. *AT&T Labs [Online]*. Available: <http://yann.lecun.com/exdb/mnist>, 2, 2010.
- [16] Y. Lu and F. M. Salem. Simplified gating in long short-term memory (lstm) recurrent neural networks. *arXiv:1701.03441*, 2017.
- [17] T. Mikolov, A. Joulin, S. Chopra, M. Mathieu, and M. Ranzato. Learning longer memory in recurrent neural networks. *arXiv preprint arXiv:1412.7753*, 2014.
- [18] R. Pascanu, T. Mikolov, and Y. Bengio. On the difficulty of training recurrent neural networks. *ICML (3)*, 28:1310–1318, 2013.
- [19] F. M. Salem. A basic recurrent neural network model. *arXiv preprint arXiv:1612.09022*, 2016.
- [20] F. M. Salem. Reduced parameterization in gated recurrent neural networks. Technical Report 11-2016, MSU, 2016.
- [21] F. M. Salem. Slim lstms. *arXiv preprint arXiv:1812.11391*, 2018.
- [22] W. Zaremba. An empirical exploration of recurrent network architectures. *An empirical exploration of recurrent network architectures*, 2015.
- [23] W. Zaremba, I. Sutskever, and O. Vinyals. Recurrent neural network regularization. *arXiv preprint arXiv:1409.2329*, 2014.